Heterocyst patterns without patterning proteins in cyanobacterial filaments

Jun F. Allard [a], Alison L. Hill [b], Andrew D. Rutenberg [a],*

[a] *Department of Physics and Atmospheric Science, Dalhousie University, Halifax, Nova Scotia, Canada B3H 1Z9*
[b] *Department of Physics, Queen's University, Kingston Ontario, Canada K7L 3N6*

Abstract

We have quantitatively modeled heterocyst differentiation after fixed nitrogen step-down in the filamentous cyanobacterium *Anabaena* sp. PCC 7120 without lateral inhibition due to the patterning proteins PatS or HetN. We use cell growth and division together with fixed-nitrogen dynamics and allow heterocysts to differentiate upon the local exhaustion of available fixed nitrogen. Slow transport of fixed nitrogen along a shared periplasmic space allows for fast growing cells to differentiate ahead of their neighbors. Cell-to-cell variability in growth rate determines the initial heterocyst pattern. Early release of fixed nitrogen from committed heterocysts allows a significant fraction of vegetative cells to be retained at later times. We recover the experimental heterocyst spacing distributions and cluster size distributions of Khudyakov and Golden [Khudyakov, I.Y., Golden, J.W., 2004. Different functions of HetR, a master regulator of heterocyst differentiation in *Anabaena* sp PCC 7120, can be separated by mutation. Proc. Natl. Acad. Sci. U. S. A. 101, 16040–16045].
© 2007 Elsevier Inc. All rights reserved.

Keywords: Filamentous cyanobacteria; Anabaena; Heterocyst commitment; Lateral inhibition; Fixed nitrogen; Diazotrophic; Differentiation; Computational modeling; Pattern formation; Growth and division

Introduction

The filamentous cyanobacterium *Anabaena/Nostoc* sp. strain PCC 7120 develops heterocysts in response to environments lacking a source of fixed nitrogen (for recent reviews see Meeks and Elhai (2002), Golden and Yoon (2003), Flores and Herrero (2005), and Zhang et al. (2006)). It is a geometrically simple and important model system showing multicellular development. Within a filament, the terminally differentiated heterocysts fix atmospheric nitrogen for the remaining vegetative cells. A regular pattern of differentiation is observed, with approximately one cell in ten becoming a heterocyst.

The paradigm of diffusible inhibitors and promoters of morphogenesis ("morphogens") dates back to Turing (1952). One basic question is what are the diffusible morphogens? A second question is how does the spatial pattern initially arise? For filamentous cyanobacteria, key patterning proteins in the development of heterocyst patterns, such as HetR, PatS, and HetN, have been identified. HetR (Buikema and Haselkorn, 2001; Huang et al., 2004) is a non-diffusing "master regulator" of heterocyst differentiation that begins to be expressed immediately after a step-down of fixed nitrogen and is quickly localized to clusters of "proheterocysts". HetR promotes the expression of *patS*, which is believed to encode or activate a diffusible inhibitor of differentiation (Yoon and Golden, 1998; Yoon and Golden, 2001). In wild-type (WT) filaments, PatS causes most proheterocysts to revert into vegetative cells—leaving isolated heterocysts. Proheterocysts can also be reverted by the addition of fixed nitrogen. HetN inhibits the expression of *hetR* (Li et al., 2002; Callahan and Buikema, 2001) and also acts as an inhibitor of heterocyst differentiation. While PatS and HetN influence heterocyst patterns, it is not known how the global deprivation of fixed nitrogen is *initially* translated into differentiation of some cells and not others.

Recent experiments by Khudyakov and Golden (2004), herein KG, have identified a single point mutation in *hetR*, resulting in the protein $HetR_{R223W}$ that is relatively insensitive to the effects of either PatS or HetN, but still competent to promote heterocyst differentiation. The resulting heterocyst

* Corresponding author. Fax: +1 902 494 5191.
E-mail address: andrew.rutenberg@dal.ca (A.D. Rutenberg).

spacing distribution 48 h after nitrogen step-down appears qualitatively random, apart from a strong bias towards even numbers of intervening vegetative cells between heterocysts that is attributed to cell division after heterocyst commitment.

Wolk and Quine (1975) modeled heterocyst differentiation in WT filaments by sequentially and randomly placing heterocysts that locally suppressed subsequent heterocyst placement. To try to explain the KG results we first consider such a "random initiation" model but with no diffusible inhibitors. This corresponds to a global trigger of heterocyst differentiation following fixed-nitrogen deprivation followed by cell growth and division.

Fogg (1949) speculated that heterocyst positions are determined by local levels of a nitrogenous inhibiting substance ("fixed nitrogen"). We explore the viability of that hypothesis by modeling how *local* concentrations of fixed nitrogen within the cyanobacterial filament may determine the observed patterns of heterocysts in the KG HetR$_{R223W}$ system. We include cell growth and division, as well as production, transport, and consumption of fixed nitrogen within the filament. We do not include any explicit effects of inhibiting proteins PatS or HetN.

Three key assumptions underlie our quantitative model. The first is that heterocyst commitment occurs when a cell becomes starved of available fixed nitrogen. As discussed by KG, this assumption appears reasonable for the HetR$_{R223W}$ mutant in light of its late differentiation after fixed-nitrogen step-down and the relatively low levels of exogenous fixed nitrogen needed to revert proheterocysts compared to WT. The second assumption is that randomness is introduced into the heterocyst differentiation process primarily through the variation of the time-to-division in individual cells. Indeed, we find that the experimental variation of time-to-division is sufficient as the *only* source of randomness or stochasticity in our model. The third assumption is that fixed nitrogen can be released from committed heterocysts *before* they have completed their differentiation and started to fix atmospheric nitrogen. This early fixed-nitrogen release could be provided by catabolism of reservoirs of cyanophycin (Picossi et al., 2004) or by the proteolysis of phycobiliprotein that is observed upon heterocyst commitment (Wood and Haselkorn, 1980).

Models and methods

Random growth and division

Cells are indexed with a number $i \in [1, n]$, where $n(t)$ is the number of cells at time t. Upon cell division two daughter cells are inserted into the filament at the parent cell location. Since newly divided cells in *Anabaena* sp. PCC 7120 are all approximately the same size (Meeks and Elhai, 2002) we start every vegetative cell at a fixed size, $M=1$, and let it grow at a constant rate before dividing it symmetrically at $M=2$:

$$dM(i,t)/dt = 1/T_i \qquad (1)$$

(The volume of the cell is $M(i,t)v_V$, where v_V is a constant.) The time-to-division, T_i is randomly selected for each cell i at its birth from a symmetric triangular distribution with mean T_D and limits $T_D(1 \pm \phi)$. (Qualitatively similar results are found using a uniform distribution.) The parameter $\phi \in [0, 1]$ controls the amount of randomness in the growth process.

We obtained video of diazotrophically growing filaments (provided by James Golden) corresponding to the strain and growth conditions of the HetR$_{R223W}$ heterocyst spacing data (Khudyakov and Golden, 2004). The video has a duration of 61 h and includes approximately 290 cells in the field of view when the video begins. We tracked the 26 individual cells that were visible for their entire birth to division cycle, where division is indicated by a clearly visible septum between daughter cells, to estimate T_D and ϕ.

Random initiation model

To explore the possibility that growth and division alone may be sufficient to explain the experimental heterocyst patterns in the HetR$_{R223W}$ system, we start with $n=8$ cells and allow them to grow and divide, following Eq. (1), until we reach $n=10^4$ at which time we randomly change a fraction ρ of vegetative cells into heterocysts. After a time interval ΔT_H of further growth and division, we analyze the cluster spacings from the middle third of the filament (to avoid end effects). This random initiation corresponds to some *global* response to fixed-nitrogen shortage in the filament, without the inhibitory mechanisms of earlier quantitative random initiation models (Wolk and Quine, 1975).

We have examined 10^5 parameterizations randomly chosen log-uniformly from plausible parameter ranges of $\rho \in [0.1, 0.99]$, $\Delta T_H/T_D \in [0.1, 2.0]$, and $\phi \in [0.10, 0.99]$ to optimize the p-value of a χ^2 test comparing the distributions of contiguous vegetative and heterocysts with the experimental KG distributions shown in Figs. 2A and D. We additionally examined 10^5 parameter sets by locally moving in parameter space to maximize the p-value, starting with 30 randomly chosen parameter sets in the above interval.

Fixed-nitrogen model

Fixed nitrogen is essential for cell function, however in diazotrophic conditions it is only produced in significant quantities in heterocysts in the form of, e.g., glutamine (Thomas et al., 1977; Flores and Herrero, 2005). The fixed nitrogen is thought to diffuse, possibly associated with periplasmic binding proteins (PBP) to prevent release into the extracellular medium (Montesinos et al., 1995), through a common periplasmic space (Flores et al., 2006) to the vegetative cells. We model the exchange of fixed nitrogen between cells and the periplasm and its diffusion within the periplasmic space. We also model the sources of fixed nitrogen (heterocysts) and the sinks (vegetative cells).

We assume that the primary need for fixed nitrogen is vegetative cell growth, so that vegetative cells consume fixed nitrogen at a rate proportional to their rate of growth, $1/T_i$. We denote the vegetative cytoplasmic and the periplasmic amounts of fixed nitrogen by N_V and N_P, respectively. Then our dynamics, shown schematically in Fig. 1, are given by

$$dN_V(i,t)/dt = (D_I N_P(i,t)/v_P - D_O N_V(i,t)/v_V)/M(i,t) - \eta v_V/T_i \qquad (2)$$

$$dN_P(i,t)/dt = D_P \nabla^2 (N_P/M)/v_P$$
$$+ \begin{cases} (D_O N_V(i,t)/v_V - D_I N_P(i,t)/v_P)/M(i,t) & (3a) \\ H_{EARLY} & (3b) \\ H & (3c) \end{cases} \qquad (3)$$

where Eq. (2) applies to the cytoplasm of vegetative cells, Eq. (3a) applies to the periplasmic compartments of vegetative cells, Eq. (3b) applies to the periplasm of heterocysts within a time τ_H of commitment, and Eq. (3c) applies to the periplasm of mature heterocysts. The volume of a newly divided vegetative cell's cytoplasm and its corresponding periplasm are given by the constants v_V and v_P, respectively, and η is the amount of fixed nitrogen needed per cubic micron of cell growth. The discrete Laplacian $\nabla^2 (N_P/M) \equiv N_P(i+1,t)/M(i+1,t) - 2N_P(i,t)/M(i,t) + N_P(i-1,t)/M(i-1,t)$ governs diffusion through the periplasm. We do not allow fixed-nitrogen transport between the periplasmic spaces of adjacent heterocysts, though we obtain qualitatively similar results if we do. We allow for the possibility of *export* of available fixed nitrogen from vegetative cells (D_O) in addition to import (D_I). On cell division, fixed nitrogen is divided equally between the two daughter cells.

The differentiation of heterocysts in the mutant HetR$_{R223W}$ strain is inhibited by very low levels of exogenous fixed nitrogen compared to WT (Khudyakov
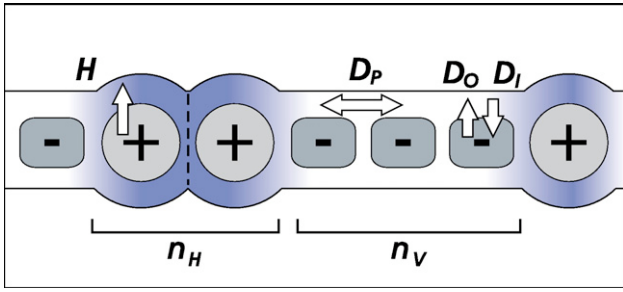
Fig. 1. Qualitative illustration of fixed-nitrogen dynamics within our model. Heterocysts, indicated by circles, are sources of fixed nitrogen ("+") and export it into the periplasm (H_{EARLY} then H). Vegetative cells are sinks ("−") and import fixed nitrogen from the periplasm (D_I). Export of fixed nitrogen from vegetative cells to the periplasm is also allowed (D_O). Diffusion of fixed nitrogen along the periplasm is included (D_P), though no diffusion is allowed between adjacent heterocysts (dashed line). The resulting gradients of fixed nitrogen are qualitatively indicated by the gradient shading, though in the model the periplasmic space is discretized into bins adjacent to individual cells. Contiguous clusters of n_V vegetative cells and n_H heterocysts are indicated. Frequency distributions of these cluster sizes are shown in Fig. 2.

and Golden, 2004). We incorporate this in our model: when $N_V(i,t)=0$, the ith cell irreversibly commits to heterocyst differentiation. Our model also includes the possibility of immediate release of fixed nitrogen from committed heterocysts at a rate H_{EARLY}, until newly fixed nitrogen can be exported at a rate H after a time τ_H following commitment.

To implement our model, we first divide all nitrogen amounts by a factor of ηv_V so that the proportionality factor of the consumption rate is unity in Eq. (2). We also absorb scale factors in transport coefficients to obtain a simplified computational model:

$$d\tilde{N}_V(i,t)/dt = (\tilde{D}_I\tilde{N}_P(i,t) - \tilde{D}_O\tilde{N}_V(i,t))/M(i,t) - 1/T_i \quad (4)$$

$$d\tilde{N}_P(i,t)/dt = \tilde{D}_P\nabla^2(\tilde{N}_P(i,t)/M(i,t)) + \begin{cases} (\tilde{D}_O\tilde{N}_V(i,t) - \tilde{D}_I\tilde{N}_P(i,t))/M(i,t) & (5a) \\ \tilde{H}_{EARLY} & (5b) \\ \tilde{H} & (5c) \end{cases} \quad (5)$$

where Eqs. (5a), (5b), and (5c) correspond to the periplasmic components of vegetative, committed heterocysts, and mature heterocysts, respectively. Rescaled parameters are related to physiological parameters by $N_V=\eta v_V \tilde{N}_V$, $N_P=\eta v_V \tilde{N}_P$, $H_{EARLY}\equiv\eta v_V \tilde{H}_{EARLY}$, $H\equiv\eta v_V\tilde{H}$, $D_I\equiv v_P\tilde{D}_I$, $D_P\equiv v_P\tilde{D}_P$ and $D_O\equiv v_V\tilde{D}_O$. The effective periplasmic diffusivity is given by $\tilde{D}_PL v_P/A_P=\tilde{D}_PL^2$, where A_P is the cross-sectional area of the periplasm and L is the cell length.

We start each model filament with $n=8$ cells, each of which has random M_i and T_i, and let it grow and divide by numerically integrating Eq. (1) and Eqs. (4) (5). During this initial growth, when $t<0$, we approximate the connection between the periplasm and the nitrogen-rich extracellular space by fixing the value of the periplasmic fixed-nitrogen at each cell, $\tilde{N}_P(i)=\tilde{N}_f\equiv f[\tilde{D}_O/\tilde{D}_I+1/(\tilde{D}_IT_D(1-\phi))]$. The parameter f (and hence $\tilde{N}_f$) is chosen high enough that no cells differentiate into heterocysts while $t<0$. When the filament has reached at least $n=10^4$ cells at $t=0$, by which time it has steady-state distributions of T_i and M_i, the periplasmic constraint is released to reflect the change to diazotrophic growth conditions. At $t=48$ h we extract heterocyst and vegetative cluster size statistics from the middle third of the filament.

Parameter determination for the fixed-nitrogen model

We first examined at least 1000 parameter sets log-uniformly chosen from plausible parameter ranges, as shown in Table 1. Starting with the 10 best parameterizations (with highest p-values), we ran independent refining searches to further optimize the p-value of a χ^2 test comparing the distributions of contiguous vegetative and heterocysts with the experimental distributions

shown in Figs. 2A and D. Trial parameterizations were generated by randomly scaling each parameter by a small factor (between 1.2 and 2) and the new parameterization was accepted by a simulated annealing algorithm with fixed temperatures T_{SA} (Kirkpatrick et al., 1983) on the basis of the χ^2. The refining searches explored at least 100 parameterizations each with $T_{SA}=10$, and at least 100 further parameterizations each with $T_{SA}=1$. All parameter sets with $p\geq0.1$ were examined once more to reduce stochastic fluctuations. Those parameter sets that recovered $p\geq0.1$ were used to determine acceptable parameter ranges. A parameter set with $p>0.5$ was selected with parameters toward the middle of the acceptable parameter ranges, and it was run 20 additional times to accumulate heterocyst cluster and commitment statistics.

Additional constraints have been imposed on our parameters to make our search for viable parameterizations more efficient. The steady-state heterocyst fraction in WT is approximately 10% (Yoon and Golden, 1998). Since we expect that the HetR$_{R223W}$ mutant will not significantly affect fixed-nitrogen production or consumption compared with WT, we balance production with consumption via. $\rho\tilde{H}=(1-\rho)\langle 1/T_i\rangle$ (where the angle brackets indicate an average value). With small ϕ, we obtain $\tilde{H}T_D\approx 9$ and impose $\tilde{H}T_D\in[5, 20]$. We also impose $T_D\in[20, 80]$ (hours) and $\phi\in[0.1, 0.9]$ corresponding to the experimental growth data (see below), and $\tau_H\in[6, 24]$ (hours) corresponding to the delay until complete heterocyst differentiation after commitment (Yoon and Golden, 1998). We also insist that any early release of fixed nitrogen before *de novo* fixation in committed heterocysts is not more than was incorporated during vegetative growth, i.e. $\tilde{H}_{EARLY}\tau_H<1$.

Results

Experimental time to division

From the analysis of the experimental video, we find that the mean time to division is $T_D=38\pm2$ h (where the uncertainty indicates the standard error of the estimate) with a significant standard deviation of 8 h for vegetative cells of *Anabaena/Nostoc* sp. PCC 7120 HetR$_{R223W}$. Since the standard deviation of the T_i for our triangular distribution is $\phi T_D/\sqrt{6}$ we estimate $\phi\approx 0.5\pm0.1$. Our model's triangular distribution is qualitatively consistent with the data.

Random initiation model does not recover initial heterocyst pattern

Of the 2×10^5 parameter sets considered, 343 had $p\geq0.001$ in the initial run and had 20 additional runs each to independently determine the average p-values. We do not find any

Table 1

Model parameter [a] (units)	Initial range [b]	Acceptable range [c]	Example value [d]
T_D (h)	[20, 80]	[23, 41]	27.9
ϕ	[0.1, 0.9]	[0.1, 0.3]	0.237
$\tilde{D}_I$ (h^{-1})	[1, 1000]	[0.9, 16]	3.06
$\tilde{D}_O$ (h^{-1})	[1, 1000]	[0.06, 4]	0.496
$\tilde{D}_I/\tilde{D}_O$	n/a	[2.5, 37]	6.2
$\tilde{D}_P$ (h^{-1})	[1, 1000]	[600, 10,500]	4968
$\tilde{H}_{EARLY}$ (h^{-1})	[0.01, 0.2]	[0.03, 0.07]	0.0379
$\tilde{H}$ (h^{-1})	[0.1, 1]	[0.2, 0.6]	0.424
τ_H (h)	[6, 24]	[6, 23]	16.5
F	[0.01, 10]	[0.06, 0.9]	0.425

[a] For the fixed-nitrogen model.
[b] Not used as constraints.
[c] From 92 parameter sets that have $p\geq0.1$.
[d] This parameterization has $\langle p\rangle=0.63$ and is used for Figs. 2C, F, and 3.
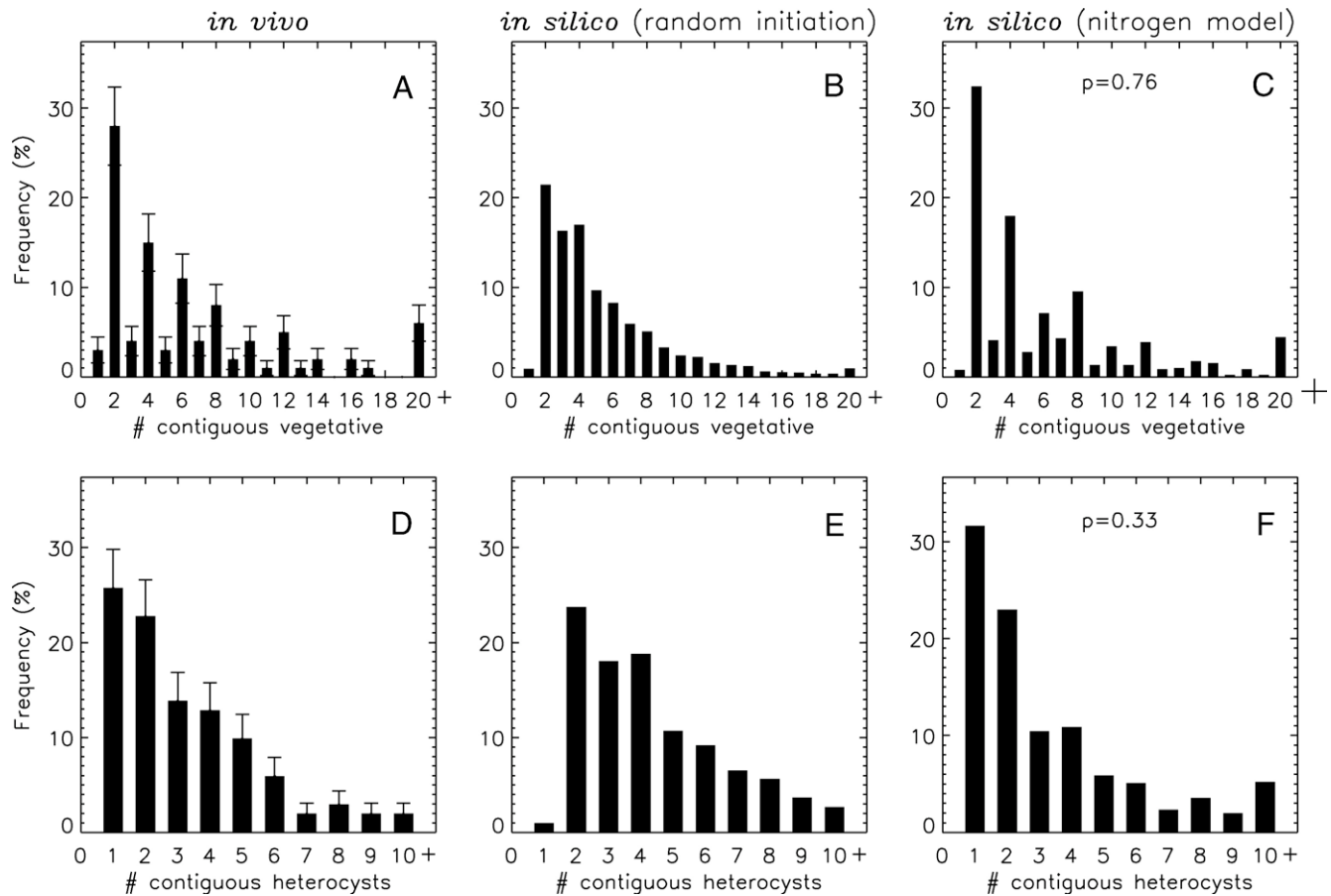
Fig. 2. Distributions of sizes of vegetative cell clusters at $t=48$ h after fixed-nitrogen step-down for (A) experiment (Khudyakov and Golden, 2004), (B) the best random initiation model with growth and division, and (C) our fixed-nitrogen model. Corresponding distributions of heterocyst clusters at $t=48$ h for (D) experiment, (E) the random initiation model, and (F) our fixed-nitrogen model. Twenty independent model runs were used for the model data, with 24,170 intervals used for panels B and E and 9010 intervals for panels C and F. Error bars on the *in vivo* data represent uncertainties using the experimental distributions and 147 and 155 experimental intervals, respectively, for panels A and D (I. Y. Khudyakov, private communication).

significant agreement with experiment. In Figs. 2B and E we show the distributions for the best parameter set of our basic random initiation model ($\rho=0.595$, $\phi=0.990$, and $\Delta T_H/T_D = 1.58$, with $\langle p \rangle = 4 \times 10^{-6}$). Note that the absence of an odd–even effect for larger vegetative cluster sizes in Fig. 2B reflects the lack of synchronization of cell division due to the large ϕ.

Fixed-nitrogen model consistent with experimental patterns

At least half of the refining searches obtained significant parameterizations with $p \geq 0.1$. The other searches were significantly slowed by small time-steps necessitated by large transport coefficients. Overall, over 14,000 parameterizations were explored and 92 parameterizations were found with $p \geq 0.1$, 22 of which had $p \geq 0.5$. Those "acceptable" sets that recovered $p \geq 0.1$ or $p \geq 0.5$ when rerun were well clustered in parameter space (see Supplementary Fig. 4 for scatter plots). The parameter ranges with $p \geq 0.1$ are given in Table 1. One of the better parameterizations, with $\langle p \rangle = 0.63$, shown in Table 1 and indicated by a red circle in Fig. 4 was used to generate Figs. 2C, F, and 3.

The acceptable parameterizations of our model have significant rates of export (D_O), as well as of import (D_I) of avail-

able fixed nitrogen from vegetative cells, with a significant correlation between the import and export rates. Early export of fixed nitrogen from heterocysts, $\tilde{H}_{EARLY}$, is always significant for acceptable parameterizations but remains small compared to $\tilde{H}$.

Commitment correlation with cell cycle

Histograms of the distributions of cell mass M_i and time-to-division T_i at the time of heterocyst commitment are shown in Fig. 3. While cells of all $M_i \in [1, 2]$ and $T_i \in [T_D (1-\phi), T_D (1+\phi)]$ are represented, the distributions are significantly shifted towards smaller M_i and faster growing cells with small T_i.

Late-time pattern not fully recovered

At $t=48$ h we find a 35% heterocyst fraction, in agreement with experiment (Khudyakov and Golden, 2004). These excess heterocysts compared to the steady-state fraction of Yoon and Golden (1998) result in excess fixed-nitrogen production along the filament. As a result, our model shows very little heterocyst differentiation for a long time after $t=48$ h. Under the appro-
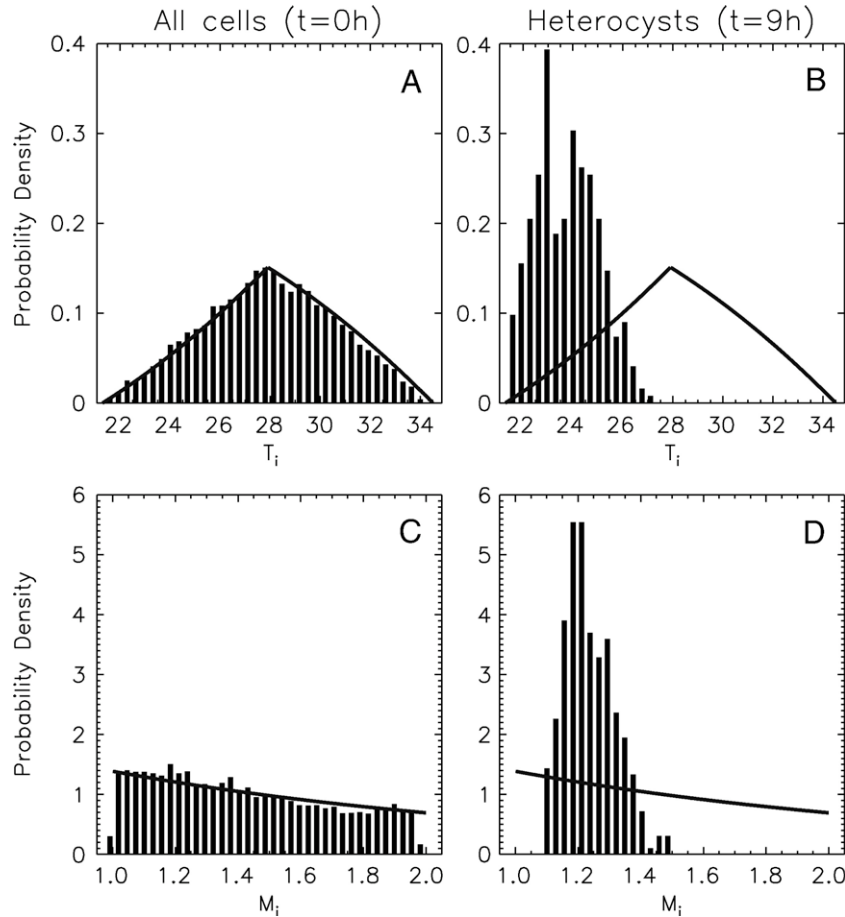
Fig. 3. The distribution of cell time-to-division T_i and cell size M_i before deprivation (A and C, respectively) and 9 h after cell differentiation begins for cells committing to become heterocysts at the time of commitment (B and D, respectively). From Eq. (2), the rate of consumption of fixed nitrogen is proportional to $1/T_i$ and so smaller T_i leads to faster local consumption of fixed nitrogen and thus earlier differentiation. The triangular distribution used to determine T_i for all cells at birth is recovered in panel A, with a bias towards cells with higher T_i since a longer lifetime increases a cell's chance of being sampled at a given time. After differentiation begins, cells that commit to become heterocysts show a significant bias towards faster growing cells, corresponding to smaller T_i, as seen by comparing (B) with (A). The analytically predicted steady-state distribution of cell masses (see Powell (1956)) is shown as a solid line in panels C and D. The steady-state distribution of time-to-division T_i, shown as a solid line in panels A and B, results from a convolution of the imposed triangular distribution at division with the steady-state distribution of cell masses. As seen in panels A and C, the *in silico* distribution agrees with the analytic prediction until heterocyst commitment occurs, at which time there is a bias towards differentiation of younger and smaller cells into heterocysts (D).

ximation that there is no heterocyst differentiation between $t=48$ and $t=144$ h, one would expect the heterocyst cluster sizes to remain unchanged in that time interval. We do observe this (data not shown) both in our model and, with a significance of 61%, in the experimental distributions (Khudyakov and Golden, 2004). However our model does not recover the experimental *vegetative* cluster size distribution at $t=144$ h.

Discussion

The reliably significant *p*-values obtained for our fixed-nitrogen model, which includes random growth and division, fixed-nitrogen dynamics, and heterocyst commitment upon available fixed-nitrogen starvation, indicate that it accurately reproduces the observed experimental heterocyst spacing distributions as measured at $t=48$ h after fixed-nitrogen step-down for the filamentous cyanobacterium *Anabaena* sp. PCC 7120 with HetR$_{R223W}$ (Khudyakov and Golden, 2004), as shown in Fig. 2. The model correctly recovers the occasional

large vegetative clusters seen experimentally, but at the same time the occasional large heterocyst clusters. Growth and division also recover the pronounced odd–even effect in the heterocyst spacing histograms, as suggested by KG. In contrast, global random initiation of heterocyst commitment is inconsistent with the experimental heterocyst distributions for HetR$_{R223W}$.

In our detailed model, inhomogeneities of fixed nitrogen along the cyanobacterial filament are important in the initiation of the heterocyst pattern. The random distribution of growth rates of individual vegetative cells, which is observed experimentally, provides sufficient inhomogeneities for heterocyst selection given the relatively slow periplasmic transport. The resulting lack of fixed nitrogen due to local sinks acts as a promoter of heterocyst differentiation (through the local action of 2-oxoglutarate and *ntcA* (Zhang et al., 2006)). After heterocysts commit to differentiate, the export of fixed nitrogen leads to a spatially graded inhibition of nearby heterocysts.

The acceptable ($p \geq 0.1$) parameter range of the time-to-division from our detailed model, $T_D \in [23, 41]$, overlaps with the independently determined experimental value (see Models and methods) of $T_D = 38 \pm 2$ h. Both overlap with a reported range of 15–48 h for various *Nostoc* species and growth conditions (Meeks and Elhai, 2002). The parameter range for the randomness parameter $\phi \in [0.1, 0.3]$ is slightly below our experimental estimate ($\phi \approx 0.5 \pm 0.1$). This difference could be explained by some anticorrelation between the time-to-division of nearby cells, which would reduce the impact of large or small growth rates for individual cells. Unfortunately, the video data used to estimate T_D and ϕ are not sufficient to explore such correlations of division times.

The observation of a shared periplasmic space in *Anabaena* sp. PCC 7120 (Flores et al., 2006) suggests that periplasmic diffusion is the mechanism for intercellular fixed-nitrogen transport observed during diazotrophic growth (Montesinos et al., 1995; Wolk et al., 1974; Van Gorkom and Donze, 1971). Supporting this, we find that we can only recover the experimental cluster distributions with parameters corresponding to periplasmic transport, with $\tilde{D}_P \gg \tilde{D}_I, \tilde{D}_O$. Our acceptable range of fixed-nitrogen transport in the periplasm, $\tilde{D}_P \in [600, 10{,}500]$ cells^2/h, corresponds to a diffusion constant range of 2.6 to 47 μm^2/s using a typical cell length $L = 4$ μm. This is significantly less than $D_{glut} \approx 650$ μm^2/s measured for glutamine in 3% agarose gels (Frazier et al., 2001), but comparable with the diffusivity of GFP, $D_{GFP} = 2.6$ μm^2/s, within the periplasm of *E. coli* (Mullineaux et al., 2006). Indeed, D_{GFP} may provide a reasonable estimate for the transport of fixed nitrogen associated with periplasmic binding proteins (PBP) within the periplasm (Quiocho and Ledvina, 1996). Fixed-nitrogen transport may also be locally modified along a filament at late times by the presence of differentiated heterocysts. Similarly, heterocysts *inside* clusters may fix nitrogen at diminished rates, compared to those at the edge of clusters (Meeks and Elhai, 2002). These effects are crudely incorporated in our model by eliminating fixed-nitrogen transport between adjacent heterocysts, though qualitatively similar results are obtained without this restriction.

The transport of fixed nitrogen in filaments of *Anabaena cylindrica* has been indirectly measured with pulse-chase experiments using ^{13}N (Wolk et al., 1974). They report an effective diffusivity of ≈ 360 cells^2/h. An independent estimate of ≈ 64 cells^2/h can be obtained (Wolk et al., 1974) from the observation of significant gradients of phycocyanin after the readmission of N_2 gas to N_2 starved filaments (Van Gorkom and Donze, 1971). These two experimental results do not overlap, indicating significant experimental uncertainty, but they are both somewhat lower than our range.

The significant amplitude of $\tilde{H}_{EARLY}$ in our model indicates that early release of fixed nitrogen may occur from committed heterocysts long before the 12-hour delay (Yoon and Golden, 2001) after which a morphologically mature heterocyst begins to fix atmospheric nitrogen. This early release of fixed nitrogen from committed heterocysts is only approximately one tenth the rate from morphologically mature heterocysts ($\tilde{H}$), however it is essential to support ongoing vegetative growth during the lengthy time interval of heterocyst development. Early export

could be supplied by proteolysis of their photosynthetic machinery (Meeks and Elhai, 2002), such as phycobiliprotein within committed heterocysts. Catabolism of fixed-nitrogen reservoirs in the form of cyanophycin (Picossi et al., 2004) is also possible. These sources have the potential to liberate significant amounts of fixed nitrogen for uses outside the committed heterocyst. Indeed, extracellular leakage of amino acids has been observed during heterocyst differentiation (Thiel, 1990).

For vegetative cells, our acceptable parameterizations all have the export rate of fixed nitrogen approximately equal to the import rate ($D_I/D_O \equiv v_P/v_V \tilde{D}_I/\tilde{D}_O \in [0.25, 3.7]$, using $v_P/v_V \approx 10\%$ from *E. coli* (Van Wielink and Duine, 1990; Graham et al., 1991)). For vegetative cells, we accordingly expect to find a comparable number of fixed-nitrogen efflux pumps compared to uptake pumps connecting the cytoplasmic to the periplasmic space. While both export and import mechanisms are working somewhere in the filament (Flores and Herrero, 2005; Montesinos et al., 1995; Picossi et al., 2005), we hypothesize that they both operate within any given vegetative cell. The significant efflux rate (D_O) in our model reflects the necessity of supplying vegetative cells furthest from heterocysts with enough fixed nitrogen to facilitate growth given the strong fixed-nitrogen gradients along the filament. Much smaller D_O leads to hyper-accumulation of fixed nitrogen in vegetative cells immediately adjacent to heterocysts, while cells furthest from heterocysts are starved of fixed nitrogen and differentiate—leading to too many heterocysts compared to experiment. Much larger D_O leads to insufficient fixed nitrogen in the faster growing vegetative cells and hence to their differentiation and again too many heterocysts.

Our model is relatively simple. Many proteins and interactions implicitly contribute to the timescales and interactions within our model. For example, for $t < 0$ we implicitly account for available extracellular nitrogen through the fixed periplasmic value $\tilde{N}_f$, and we implicitly account for PBP in our slow periplasmic transport. Fixed-nitrogen sequestration and release are not explicit in our model, though it implicitly permits early fixed-nitrogen release upon heterocyst commitment. While glutamine production in heterocysts requires glutamate and sucrose supplied by vegetative cells (Meeks and Elhai, 2002), we do not explicitly include them in our model. Growth rates may also be dependent on the *local* fixed-nitrogen amount, $N_V(i,t)$, following the observation that exogenous levels of fixed nitrogen can affect growth rates (Fogg, 1949). We would expect that details of fixed-nitrogen sequestration and fixed-nitrogen dependent growth rates will affect the heterocyst patterns at late times and may be necessary to describe KG data at $t = 144$ h. Adding these extensions would make the model more flexible, and possibly more realistic, but at the likely cost of making it too unconstrained by the currently available experimental data.

Could our model be simpler? We believe that all of the components in our model, random growth and division, fixed-nitrogen transport in the cyanobacterial filament with sources at heterocysts and sinks at vegetative cells, and a local trigger of heterocyst differentiation, are necessary for any quantitative model of heterocyst initiation. We do not believe that a

substantially simpler model is possible, while still addressing the question of why certain cells and not others differentiate into heterocysts.

Recently, experiments have been done with *Anabaena* mutant strain UMH100 (Borthakur et al., 2005) that has wild-type *hetR* but no active *patS* and has *hetN* on a copper-inducible promoter. In comparison with the HetR$_{R223W}$ mutants of KG, UMH100 shows significant differences—including the almost total differentiation into heterocysts within 192 h of the onset of diazotrophic growth. It appears that in UMH100 heterocyst formation is not suppressed by any diffusible products of mature heterocysts. Since in growth medium with excess copper UMH100 does not develop heterocysts (Bortha-kur et al., 2005), HetN is implicated in this lack of response. We were unable to reproduce the UMH100 heterocyst clustering patterns with our model. This is not surprising given the lack of response to heterocyst products (internal fixed-nitrogen, in our model) seen experimentally in that system. In contrast, the HetR$_{R223W}$ system of KG has a decreasing heterocyst fraction with time after initial differentiation, with 33.8% at 48 h and 20.5% at 144 h (Khudyakov and Golden, 2004), indicating that heterocyst products are suppressing heterocyst formation in that system. This may indicate a significant role for HetN in the sensing of local fixed-nitrogen levels other than through direct interactions with HetR. It is also consistent with HetN being involved in fixed-nitrogen release from heterocysts, as is the sharp upturn of HetN expression *after* heterocyst commitment (Callahan and Buikema, 2001; Li et al., 2002). Indeed, the abundance of HetN in heterocysts (Li et al., 2002) supports some sort of mechanistic role for the protein, perhaps in addition to a regulatory one.

Our model appears to disagree with suggestions from the filamentous cyanobacterium *Anabaena variabilis* that fixed-nitrogen insufficiency of individual cells does not control heterocyst development (Thiel and Pratte, 2001). Studies in *A. variabilis* have concluded that glutamine alone is insufficient to suppress heterocyst differentiation (Thiel, 1990; Thiel and Leone, 1986). Certainly our model does not depend on glutamine being the main transported form of fixed nitrogen within the filament, though it does appear to be a likely candidate (Thomas et al., 1977; Flores and Herrero, 2005). To resolve this puzzle it has been proposed (Laurent et al., 2005) that exogenous glutamine may bypass the glutamine synthetase–glutamate synthase (GS-GOGAT) cycle and hence leave 2-OG levels high enough to induce heterocyst differentiation. An alter-native explanation is that glutamine does locally suppress heterocyst differentiation at sufficient concentrations but that glutamine is inhomogeneously distributed along the cyano-bacterial filament even before heterocyst differentiation begins. Glutamine could be imported into the filament (Thiel, 1990; Thiel and Leone, 1986), or produced under anoxic conditions (Thiel and Pratte, 2001), at sufficient *average* rates to support normal growth yet be insufficient locally for clusters of small fast-growing cells—leading to some heterocyst differentia-tion. Within our model, we see this for small enough values of f and hence periplasmic value $\tilde{N}_f$ in the initial conditions (with $t<0$).

Other hypotheses have been proposed for the details of how filaments translate a global fixed-nitrogen deprivation signal into local differentiation of heterocysts. For example, "selfish" models (see Wolk (1989)) have been proposed that have an input pumping rate (D_I) that increases as the fixed-nitrogen concentra-tion decreases. Following the observation by Mitchison et al. (1976) in *A. catenula* that only young cells differentiate into heterocysts, it has also been proposed that only cells at a certain point of their cell cycle differentiate upon global deprivation (Meeks and Elhai, 2002). Alternatively, it has been postulated that individual cells have randomly different stockpiles of fixed nitrogen and hence locally perceive the nitrogen step-down at different times (Meeks and Elhai, 2002). However, we find that these effects are qualitatively recovered by our model without needing to be explicitly built-in. Fixed-nitrogen export (D_O) qualitatively recovers selfish behavior of *net* fixed-nitrogen transport, cell size effects in Eq. (3) produce the cell cycle de-pendence seen in Fig. 3, and heterogeneity of locally available fixed nitrogen naturally arises from different growth rates, and hence different rates of nitrogen consumption, along the filament.

Within the Turing (1952) picture of pattern formation, fixed nitrogen is a diffusible morphogen that initially and locally inhibits heterocyst differentiation. However, strong heterogene-ities exist even in vegetative growth due to randomly distributed growth rates. As a result, we believe that the spatial pattern is already strong *in vivo* before diazotrophic conditions are initiated and does not spontaneously arise afterwards, unlike in the original Turing picture.

Our model provides a quantitatively self-consistent picture of how initial heterocyst selection can occur in cyanobacterial filaments in the absence of diffusible patterning proteins, and it is also consistent with the early time patterns of KG. We have shown how random cell growth and division can provide an origin for heterocyst patterning, not only to recover the odd–even effect of heterocyst spacings, but also to provide inhomogeneities to direct the initial heterocyst differentiation. Because our random growth and division and fixed-nitrogen dynamics should be essentially the same in WT filaments, we believe that they could be important determining factors positioning proheterocyst clusters in WT filaments as well. We hypothesize that initial heterocyst positions will be strongly correlated with fast-growing and/or small vegetative cells—as shown in Figs. 3B and D. A second hypothesis is that cells release fixed nitrogen soon after heterocyst commitment, before *de novo* synthesis of fixed nitrogen occurs, albeit at relatively small rates (10% or so) of the steady-state production. In WT filaments, this early release may help other diffusible morphogens, such as PatS, to resolve proheterocyst clusters. A third hypothesis is that there are significant fixed-nitrogen *efflux* pumps from vegetative cells operating during diazotrophic growth. None of these hypotheses depend on the detailed parameterization of our model, and all of them should be experimentally testable.

Our model leads us to a number of open questions related to fixed-nitrogen dynamics in the cyanobacterial filament. What is the actual distribution of the time-to-division T_i in cyanobacter-ial filaments? Does this distribution significantly change during diazotrophic conditions, and does it change according to the

local supply of fixed nitrogen? Are there significant correlations or anticorrelations either temporally (between parent and daughter cells) or spatially (between daughter cells) in the random component of the time-to-division? How is fixed nitrogen transported along the periplasm, and in what form? Is there significant transport between heterocysts? What are the signals that lead to sequestration and release of fixed nitrogen stores in vegetative cells both before and during diazotrophic growth? Are sucrose gradients along the cyanobacterial filament significant for determining heterocyst positioning under certain conditions? What about gradients of glutamate or 2-oxoglutarate, as opposed to glutamine? While specific answers to any of these questions would change the details of our model, we do not expect them to change its basic structure. We hope that our model emphasizes the importance of understanding how spatial gradients of metabolites such as fixed nitrogen affect patterns of heterocyst differentiation in cyanobacterial filaments.

Acknowledgments

Appendix A. Supplementary data

Supplementary data associated with this article can be found, in the online version, at doi:10.1016/j.ydbio.2007.09.045.

References

Borthakur, P.B., Orozco, C.C., Young-Robbins, S.S., Haselkorn, R., Callahan, S.M., 2005. Inactivation of *patS* and *hetN* causes lethal levels of heterocyst differentiation in the filamentous cyanobacterium *Anabaena* sp PCC 7120. Mol. Microbiol. 57, 111–123.

Buikema, W.J., Haselkorn, R., 2001. Expression of the *Anabaena hetR* gene from a copper-regulated promoter leads to heterocyst differentiation under repressing conditions. Proc. Natl. Acad. Sci. U. S. A. 98, 2729–2734.

Callahan, S.M., Buikema, W.J., 2001. The role of HetN in maintenance of the heterocyst pattern in *Anabaena* sp. PCC 7120. Mol. Micro. 40, 941–950.

Flores, E., Herrero, A., 2005. Nitrogen assimilation and nitrogen control in cyanobacteria. Biochem. Soc. Trans. 33, 164–167.

Flores, E., Herrero, A., Wolk, C.P., Maldener, I., 2006. Is the periplasm continuous in filamentous multicellular cyanobacteria? Trends Microbiol. 14, 439–443.

Fogg, G.E., 1949. Growth and heterocyst production in *Anabaena cylindrica* Lemm. Ann. Bot. 13, 241–259.

Frazier, B.L., Larmour, P., Riley, M.R., 2001. Noninvasive measurement of effective diffusivities in cell immobilization gels through use of near-infrared spectroscopy. Biotechnol. Bioeng. 72, 364–368.

Golden, J.W., Yoon, H.-S., 2003. Heterocyst development in *Anabaena*. Curr. Opin. Microbiol. 6, 557–563.

Graham, L.L., Beveridge, T.J., Nanninga, N., 1991. Periplasmic space and the concept of the periplasm. Trends Biochem. Sci. 16, 328–329.

Huang, X., Dong, Y.Q., Zhao, J.D., 2004. HetR homodimer is a DNA-binding protein required for heterocyst differentiation, and the DNA binding activity is inhibited by PatS. Proc. Natl. Acad. Sci. U. S. A. 101, 4848–4853.

Khudyakov, I.Y., Golden, J.W., 2004. Different functions of HetR, a master regulator of heterocyst differentiation in *Anabaena* sp PCC 7120, can be separated by mutation. Proc. Natl. Acad. Sci. U. S. A. 101, 16040–16045.

Kirkpatrick, S., Gelatt, C.D., Vecchi, M.P., 1983. Optimization by simulated annealing. Science 220, 671–680.

Laurent, S., Chen, H., Bédu, S., Ziarelli, F., Peng, L., Zhang, C.-C., 2005. Nonmetabolizable analogue of 2-oxoglutarate elicits heterocyst differentiation under repressive conditions in *Anabaena* sp. PCC 7120. Proc. Natl. Acad. Sci. U. S. A. 102, 9907–9912.

Li, B., Huang, X., Zhao, J., 2002. Expression of *hetN* during heterocyst differentiation and its inhibition of *hetR* up-regulation in the cyanobacterium *Anabaena* sp. PCC 7120. FEBS Lett. 517, 87–91.

Meeks, J.C., Elhai, J., 2002. Regulation of cellular differentiation in filamentous cyanobacteria in free-living and plant-associated symbiotic growth states. Micro. Mol. Biol. Rev. 66, 94–121.

Mitchison, G.J., Wilcox, M., Smith, R.J., 1976. Measurement of an inhibitory zone. Science 191, 866–868.

Montesinos, M.L., Herrero, A., Flores, E., 1995. Amino acid transport systems required for diazotrophic growth in the cyanobacterium *Anabaena* sp. strain PCC 7120. J. Bacteriol. 177, 3150–3157.

Mullineaux, C.W., Nenninger, A., Ray, N., Robinson, C., 2006. Diffusion of green fluorescent protein in three cell environments in *Escherichia coli*. J. Bacteriol. 188, 3442–3448.

Picossi, S., Valladares, A., Flores, E., Herrero, A., 2004. Nitrogen-related genes for the metabolism of cyanophycin, a bacterial nitrogen reserve polymer. J. Biol. Chem. 279, 11582–11592.

Picossi, S., Montesinos, M.L., Pernil, R., Lichtlé, C., Herrero, A., Flores, E., 2005. ABC-type neutral amino acid permease N-I is required for optimal diazotrophic growth and is repressed in the heterocysts of *Anabaena* sp. strain PCC 7120. Mol. Microbiol. 57, 1582–1592.

Powell, E.O., 1956. Growth rate and generation time of bacteria, with special reference to continuous culture. J. Gen. Microbiol. 15, 492–511.

Quiocho, F.A., Ledvina, P.S., 1996. Atomic structure and specificity of bacterial periplasmic receptors for active transport and chemotaxis: variation of common themes. Mol. Microbiol. 20, 17–25.

Thiel, T., 1990. Protein turnover and heterocyst differentiation in the cyanobacterium *Anabaena variabilis*. J. Phycol. 26, 50–54.

Thiel, T., Leone, M., 1986. Effect of glutamine on growth and heterocyst differentiation in the cyanobacterium *Anabaena variabilis*. J. Bacteriol. 168, 769–774.

Thiel, T., Pratte, B., 2001. Effect on heterocyst differentiation of nitrogen fixation in vegetative cells of the cyanobacterium *Anabaena variabilis* ATCC 29413. J. Bacteriol. 183, 280–286.

Thomas, J., Meeks, J.C., Wolk, C.P., Shaffer, P.W., Austin, S.M., 1977. Formation of glutamine from [^{13}N]ammonia, [^{13}N]dinitrogen, and [^{14}C]glutamate by heterocysts isolated from *Anabaena cylindrica*. J. Bacteriol. 129, 1545–1555.

Turing, A.M., 1952. The chemical basis of morphogenesis. Philos. Trans. R. Soc. Lond., B, Biol. Sci. 237, 37–72.

Van Gorkom, H.J., Donze, M., 1971. Localization of nitrogen fixation in *Anabaena*. Nature 234, 231–232.

Van Wielink, J.E., Duine, J.A., 1990. How big is the periplasmic space? Trends Biochem. Sci. 15, 136–137.

Wolk, C.P., 1989. Alternative models for the development of the pattern of spaced heterocysts in *Anabaena* (*Cyanophyta*). Pl. Syst. Evol. 164, 27–31.

Wolk, C.P., Quine, M.P., 1975. Formation of one-dimensional patterns by stochastic processes and by filamentous blue-green algae. Dev. Biol. 46, 370–382.

Wolk, C.P., Austin, S.M., Bortins, J., Galonsky, A., 1974. Autoradiographic localization of ^{13}N after fixation of ^{13}N-labeled nitrogen gas by a heterocyst-forming blue-green alga. J. Cell Biol. 61, 440–453.

Wood, N.B., Haselkorn, R., 1980. Control of phycobiliprotein proteolysis and heterocyst differentiation in *Anabaena*. J. Bacteriol. 141, 1375–1385.

Yoon, H.-S., Golden, J.W., 1998. Heterocyst pattern formation controlled by a diffusible peptide. Science 282, 935–938.

Yoon, H.-S., Golden, J.W., 2001. PatS and products of nitrogen fixation control heterocyst pattern. J. Bacteriol. 183, 2605–2613.

Zhang, C.-C., Laurent, S., Sakr, S., Peng, L., Bédu, S., 2006. Heterocyst differentiation and pattern formation in cyanobacteria: a chorus of signals. Mol. Microbiol. 59, 367–375.